Available online at www.sciencedirect.com
ScienceDirect
Tetrahedron
Tetrahedron 62 (2006) 9769–9777

Effect of a perfluorocyclopentene core unit on the structures and photoluminescence of fluorene- and anthracene-based compounds

Mijung Han,[a] Sooyong Lee,[a] Jonghwa Jung,[b] Ki-Min Park,[b] Soon-Ki Kwon,[b] Jaejung Ko,[c,*] Phil Ho Lee[a,*] and Youngjin Kang[a,*]

[a]*National Research Laboratory of Catalytic Organic Reaction, Division of Science Education and Department of Chemistry, Kangwon National University, Chuncheon 200-701, Republic of Korea*
[b]*Research Institute of Natural Sciences, Department of Chemistry and School of Nano & Advanced Materials Engineering and ERI, Gyeongsang National University, Chinju 660-701, Republic of Korea*
[c]*Department of Chemistry, Korea University, Jochiwon, Chungnam 339-700, Republic of Korea*

Received 7 June 2006; revised 30 June 2006; accepted 11 July 2006
Available online 17 August 2006

Abstract—A novel series of blue luminescent compounds, in which three identical functional groups, such as fluorene, anthracene, and spirobifluorene, are linked distortedly around a perfluorocyclopentene core, have been synthesized and characterized. The introduction of a perfluorocyclopentene linkage into the molecular framework leads to an enhancement of the photoluminescence (PL) efficiency and thermal stability. All compounds exhibit intense blue photoluminescence, which has been attributed to fluorene- or anthracene-based $\pi \rightarrow \pi^*$ transitions. The maximum emission wavelengths of all compounds at room temperature are in the region of 420–480 nm, with higher PL quantum efficiencies than in 9,10-diphenylanthracene. The electroluminescent (EL) properties of compound **4**, 1,2-bis(9,9′-spirobifluoren-2-yl)-3,3,-4,4,5,5-hexafluorocyclopentene, were investigated. A multilayer EL device with the configuration of ITO/2TNATA(60 nm)/NPB(20 nm)/ADN:2%-compound-**4**(35 nm)/Alq_3(20 nm)/LiF(2 nm)/Al has been successfully fabricated.

1. Introduction

Luminescent organic/organometallic materials are currently of great interest due to their various applications in photochemistry,[1] organic light-emitting diodes (OLEDs),[2] and chemical sensors for small molecules.[3] Among these organic materials, fluorene and/or anthracene-based compounds have been regarded as excellent fluorescent materials because of their ability to achieve high thermal stability as well as high photoluminescent (PL) efficiency.[4] Fluorene and/or anthracene-based compounds, in particular, are often used as emitting materials in electroluminescent (EL) devices.[5] Based on previous reports, promising low molecular weight emitter for use in OLEDs should have an appropriate HOMO/LUMO band gap as compared to those of the electron- and hole-transporting materials, high photoluminescent quantum yield (Φ_{PL}), good film-forming properties, and durability to heat during the vacuum deposition.[6] The Φ_{PL} is a major interest associated with the improvement of EL device efficiency, since the two properties are generally related.[7] With the aim of increasing PL efficiency, several approaches have been introduced. These include the attachment of strongly fluorescent units,[5j] such as anthracene, fluorene, and pyrene to the molecular framework, the extension of π-conjugation[8] and the combination of host–guest functions by energy transfer.[5i,9] Especially, the introduction of electron-withdrawing groups, such as fluoro- or cyano groups, renders a molecule with high PL efficiency by inter- or intramolecular interactions despite of the diminution of the HOMO and LUMO levels.[10] Moreover, it is well known that the fluorine groups bound to molecular frameworks enhance a molecule's thermal stability and enable it to sublime easily without decomposition.[11]

During our ongoing effort on the development of a variety of luminescent materials, we have observed that the presence of a linker between two chromophores has a remarkable influence on the thermal and photophysical properties.[12] The perfluorocyclopentene moiety as a linker was chosen for following reasons: (i) in EL devices performance using low-weight molecules, the molecules should be easily sublimed thermally stable, and have high PL efficiency, as the fabrication of these devices is generally performed by vacuum deposition at high temperature. Based on previous reports, compounds bearing fluorinated functional groups are satisfactory to these considerations. (ii) Photochromic materials, such as diarylethene, have recently attracted

Keywords: Perfluorocyclopentene; Optical properties; X-ray structure; OLEDs.
* Corresponding authors. Tel.: +82 33 250 6737; fax: +82 33 242 9598 (Y.K.); e-mail: kangy@kangwon.ac.kr

0040–4020/$ - see front matter © 2006 Elsevier Ltd. All rights reserved.
doi:10.1016/j.tet.2006.07.065

interest in view of their potential applications for visible image formation, optical data storage, and optical switching.[13] Dithienylethene derivatives were not only regarded as promising photochromic compounds, but they also showed high thermal stability and excellent fatigue-resistant properties. In diarylethene systems, the perfluorocyclopentene unit could play a key role in the alteration of confomers and photophysical properties.[13] Therefore, we expected that the combination of highly fluorescent fluorene or anthracene groups and fluorinated functional groups would be the best way to develop efficient emitting materials and satisfy above considerations. (iii) The introduction of two bulky triphenylamine moieties into the dithienylethene framework increases the population of the antiparallel conformer of the molecule, leading to higher conversion of a photocyclization reactions.[13a] Very high quantum efficiency is shown for these molecules in photocyclization reactions ($\Phi_{o\text{-}c}$), however, the study on OLED performance using their derivatives still remains scarce. Herein, we describe the results of our investigation on the preparation, structural characterization, electrochemical behavior, optical properties, and the fabrication of multilayer light-emitting devices of a series of fluorene and anthracene derivatives based on perfluorocyclopentene.

2. Result and discussion

2.1. Syntheses and structures

To develop new molecules with high fluorescence quantum efficiency, we have designed and synthesized a novel class of compounds based on diarylethene. The synthetic routes to **1**–**4** are given in Scheme 1. These compounds were prepared by the addition of octafluorocyclopentene to the corresponding lithiated compound, prepared from the reaction of a small excess of *n*-BuLi and the bromoarene at −78 °C. The standard workup and crystallization from CH_2Cl_2/hexane gives the titled compounds as pure pale yellow or colorless solids in moderate yields (69–82%). In addition, to evaluate the effect of a perfluorocyclopentene ring on structural features and photoluminescence, we have synthesized an aromatic analogue of compound **1**, compound **5**, through Pd-mediated Suzuki coupling. All compounds are stable in air and soluble in common organic solvents but only slightly soluble in hexane and pentane. The structures of **1**–**5** have been characterized by ^{1}H NMR, ^{13}C NMR, and elemental analyses, including X-ray diffraction analysis of **1** and **5**. In order for molecular organic materials to be useful in EL devices, they should be thermally and morphologically

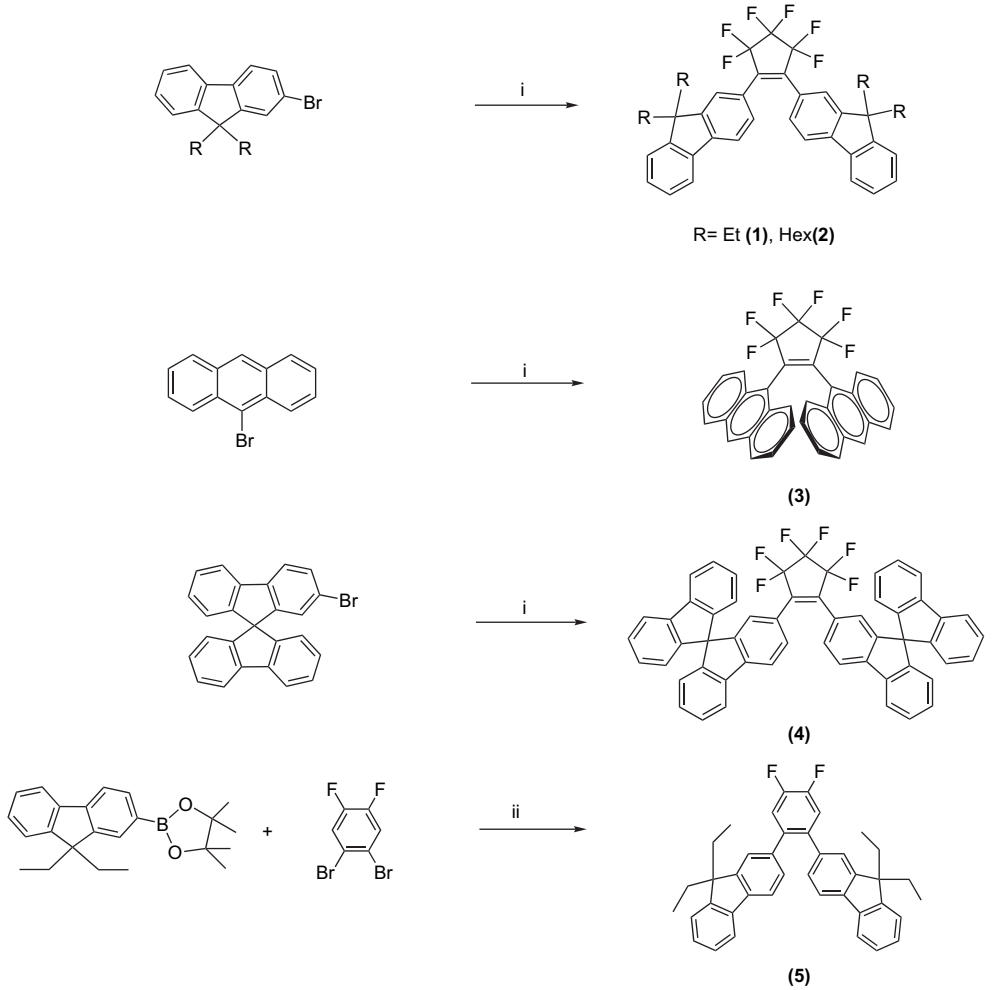

Scheme 1. Synthetic routes of **1**–**5**. Reagents and conditions: (i) *n*-BuLi/THF at −78 °C, octafluorocyclopentene (0.5 equiv); (ii) K_2CO_3, benzyltrimethylammoniumchloride, $Pd(PPh_3)_4$ (5 mol %), toluene.

Table 1. Thermal properties of **1**–**5**

Compound	T_g/°C	T_m/°C
1	—	116
2	—	93
3	—	365
4	115	273
5	—	173

stable.[17] Therefore, we performed DSC experiments to investigate the glass-transition temperatures and phase transitions for compounds **1**–**5**. Well-resolved melting transitions were observed in all cases (Table 1).

Compounds **1**–**3** did not show glass transition during either the first or second heating cycle. The melting transitions of **1**, **2**, and **3** are at 116, 93, and 365 °C, respectively. This suggests that the combination of the perfluorocyclopentene linkage and anthracene unit leads to a dramatic increase in melting transition. In contrast, the first heating cycle of **4** revealed high glass-transition temperature at 115 °C without any crystallization transition, followed by melting at 273 °C. The glass transition observed is likely attributable to a nonplanar structure and the spiro-linked bifluorene moieties of **4**. All compounds showed consistent and fully reproducible DSC diagrams during two cycles of heating and cooling, indicating that these compounds are thermally stable up to their melting points at least. The high glass-transition temperature of **4** makes it potentially useful for applications in EL devices.

To better understand the solid-state nature, single crystal X-ray diffraction analysis was conducted for **1** and **5**. Colorless crystals of **1** and **5** suitable for X-ray analysis were obtained by the slow evaporation in CH_2Cl_2 and hexane. The crystal structures and selected bond lengths and angles of **1** and **5** are presented in Figures 1 and 2, respectively.

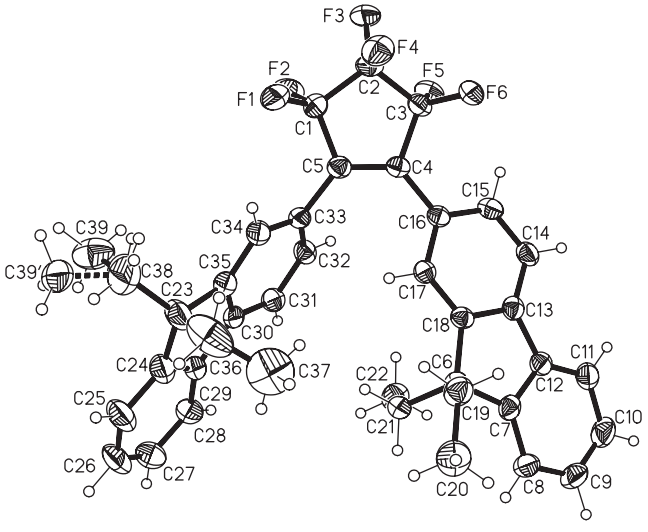

Figure 1. Molecular structure of **1** with atom labeling schemes and 50% thermal ellipsoids. Selected bond distances and angles: F(1)–C(1) 1.359(4), F(2)–C(1) 1.355(4), F(3)–C(2) 1.344(3), F(4)–C(2) 1.341(3), F(5)–C(3) 1.367(3), F(6)–C(3) 1.354(3), C(4)–C(16) 1.475(4), C(5)–C(33) 1.484(4), F(1)–C(1)–F(2) 105.8(2), F(3)–C(2)–F(4) 107.9(2), F(5)–C(3)–F(6) 105.9(2), C(16)–C(4)–C(5)–C(33) 7.5(5).

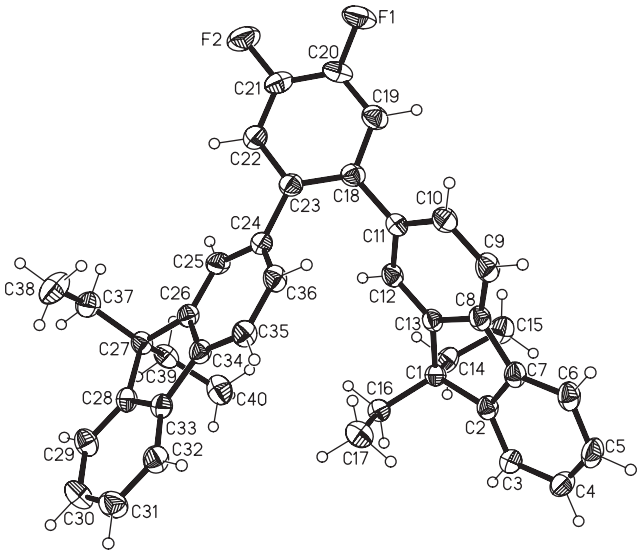

Figure 2. Molecular structure of **5** with atom labeling schemes and 50% thermal ellipsoids. Selected bond distances and angles: F(1)–C(20) 1.352(2), F(2)–C(21) 1.356(2), C(11)–C(18) 1.494(3), C(18)–C(23), 1.411(3), C(23)–C(24) 1.492(3), C(11)–C(18)–C(23)–C(24) 9.4(4).

As shown in Figure 1, two fluorene groups connected by the hexafluorocyclopentene linker in compound **1** are twisted with respect to each other, and the hexafluorocyclopentene ring is not coplanar with either of the two fluorene rings. Interestingly, the dihedral angles between hexafluorocyclopentene ring and two fluorene rings are not the same (54.3(1)° and 29.3(1)° for the C1–C5 ring and the C33 or C16 fluorene rings, respectively) and the dihedral angle between the two fluorene rings is 50.38(5)°. The nonplanarity of **1** is clearly caused by the steric hindrance between C32–H and C17–H atoms. The bond lengths C5–C33 and C4–C16 are 1.484(4) and 1.475(4) Å, respectively, and the torsion angle of C33–C5–C4–C16 is 7.5(5)°, similar to those of previously reported diarylethene compounds.[18] Compound **1** has several intermolecular interactions that appear to direct the expanded packing of the solid-state structure. The packing diagram (see Supplementary data) displays puckered 2-D sheets of molecules with slipped C–H···F intermolecular interactions (C9···F1, 3.602(4) Å; C9–H9–F1, 171.8°; C28···F2, 3.298(4) Å; C28–H28–F2, 128.4°; C15···F5, 3.305(3)Å; C15–H15–F5, 148.6°). Moreover, a F···Cπ interaction (F4···C5) also exists between two adjacent sheets, with a distance of ca. 3.160(3) Å. Additional intermolecular interactions, such as π–π stacking, were not found in the packing structure of **1**.

For compound **5**, the bond lengths of C11–C18 and C23–C24 are 1.494(3) and 1.492(3) Å, respectively, the torsion angle of C11–C18–C23–C24 is 9.4(4)°, and the dihedral angle between two fluorene rings is 54.95(3)°, which are slightly longer and larger than those of compound **1**. The differences of these values between **1** and **5** may be caused by the fact that the geometry of the linker between the two fluorene moieties changes from a pentagon to hexagon. This geometrical change leads to a reduction in the linkage angle from 72° to 60°. In contrast to **1**, the dihedral angles in **5** between the phenyl ring and the two fluorene rings are almost identical (48.82(6)° and 44.80(7)° between the phenyl ring and C11 or C24 fluorene ring, respectively). Several

intermolecular interactions are also observed in crystal packing. The distances between the carbon (C9, C12, C15C, and C32) and the fluorine (F1, F2) atoms on two adjacent molecules are in the range of approximately 2.59–2.64 Å. The packing diagram (see Supplementary data) of **5** displays a 1-D column-like structure along the *b*-axis, using the C–H···F intermolecular interactions.

Although compounds **1** and **5** have similar arrangements and intermolecular interactions in the crystal lattice, it is noteworthy that the perfluorocyclopentene ring of compound **1** has considerable conjugation with two fluorene groups, as indicated by their much smaller dihedral angles (29.3(1)°–35.7(1)°) with the perfluorocyclopentene ring relative to those of compound **5**. Both compounds **1** and **5** have interesting spatial arrangements in the crystal lattice. The fluorene groups linked by cyclopentene are oriented in the same direction, despite the presence of bulky alkyl groups at the fluorene 9-position.

2.2. Optical and electrochemical properties

The absorption and photoluminescence spectra in dilute solution and in the solid state (thin film) are depicted in Figures 3 and 4, respectively. Table 2 summarizes the optical data of **1**–**5**.

The optical band gaps of all compounds were determined by their corresponding absorption threshold in thin films. UV–vis spectra of **1**, **2**, and **4** exhibit intense absorption band between 250 and 400 nm (ε>23,800 $mol^{-1}\,dm^3\,cm^{-1}$), indicating that the electronic transitions are mostly fluorene-centered π–π*. For compound **3**, the absorption spectrum exhibits the characteristic vibrational pattern of the isolated anthracene group at 353, 370, and 409 nm. The absorption patterns of **1**, **2**, and **4** are similar in the 280–450 nm region. To examine the effect of the perfluorocyclopentene linkage on the electronic transition, we measured the absorption spectrum of **5**, in which perfluorocyclopentene is replaced by 1,2-difluorobenzene, under the same conditions. Interestingly, the maximum peak observed for **5** exhibits a significant blue shift (λ_{max}=392 nm) relative to those of **1**, **2**, and **4**. In addition, the UV edge in **5** appears at much higher energy than in **1**, **2**, and **4**. This result can be explained by strong π(fluorene) conjugation associated with π(perfluorocyclopentene) in **1**, **2**, and **4**. Considering these observations,

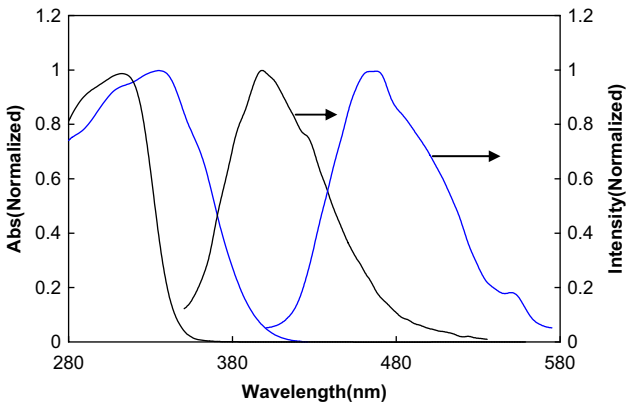

Figure 3. Absorption and emission spectra of **1** and **5** in CH_2Cl_2 at room temperature; compound **1** (blue), compound **5** (black), respectively.

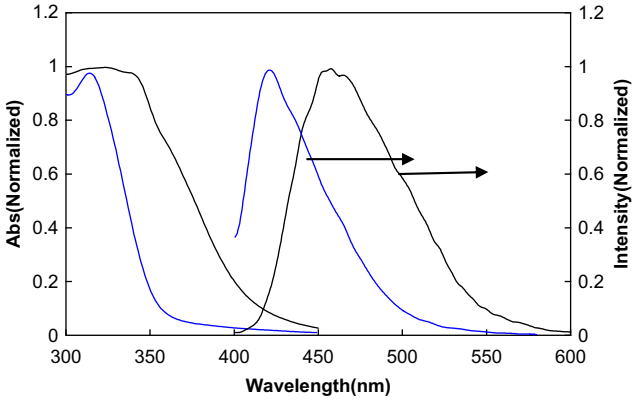

Figure 4. Absorption and emission spectra of **1** and **5** in thin film at room temperature; compound **1** (blue), compound **5** (black), respectively.

Table 2. Optical and electrochemical data for **1**–**5**

Compound	λ_{abs} (nm)		λ_{PL} (nm)		Φ_{PL}	E_g^{opt} (eV)
	Solution	Film	Solution	Film		
1	332, 353	323	455	458	>0.95	3.06
2	335	321	451	456	>0.95	3.19
3	353, 370, 392	362, 383, 409	421	501	0.41	2.76
4	328	309	459	461	0.90	3.09
5	312	314	392	421	>0.95	3.50

perfluorocyclopentene unit has a significant effect on the electronic transition energies. The emission spectra of compounds **1**–**5** in solution and as thin films at room temperature are dominated by fluorescence in the region of 400–550 nm, as supported by less than 1 ns lifetime in excited state. The emissions of all compounds in thin films, prepared by spin coating from a CH_2Cl_2/toluene solution onto a quartz plate, exhibit red-shifts of 5–20 nm to those in dilute solution. These red-shifts observed in the solid state are likely attributable to the difference in dielectric constant of the environment.[19] For compounds **1**, **2**, and **4**, the λ_{max} values of emission spectra in both solution and thin films are similar (~460 nm in thin films), and still red-shifted relative to **5**. This result can be also explained by correlating the electronic and structural effects due to the perfluorocyclopentene unit. To further investigate the electronic effects caused by the addition of perfluorocyclopentene unit, cyclic votammetry experiments were carried out using ferrocene (Fc/Fc^+) as the internal standard. Due to the limited range available in CH_2Cl_2, and inability of our instrument to measure reliable reduction potentials in the range of −2.4 to −3.5 V, we have obtained only the reliable oxidation potentials for **1** and **5**. The electrochemical behavior in aryl-substituted fluorene analogues has been described such that the irreversible oxidative and reductive processes involve the fluorene and various aryl-substituents, respectively.[4] Molecular orbital calculations for **1** and **5** provide evidence that the HOMO levels are mostly due to fluorene-based π-orbitals involving some π-orbital contributions from the linker. Upon the anodic sweep in a solvent mixture of CH_2Cl_2 and CH_3CN, irreversible oxidations are observed at 0.86 and 0.89 V for **1** and **5**, respectively. However, similar onset potentials of **1** and **5** appear at 0.75 and 0.74 V, respectively (see Supplementary data). These electrochemical behaviors indicate that the electron-withdrawing effect from the

perfluorocyclopentene unit does not have a significant influence on the HOMO energy levels, as compared to 1,2-difluorobenzene. The reductive process of the fluorene derivatives was also shown to be due to the fluorine, and is affected by the various substituents bound to the fluorene moiety. More effective conjugation stabilizes the LUMO, leading to a decreased reduction potential. Although we could not observe the reductive process, the reduction potential of **1** should be lower relative to compound **5**, as supported by the structural data and the optical absorption threshold. Another fact affecting the nature of the luminescence in molecular materials is intermolecular interactions in the solid state. There were F···Cπ interactions in crystal packing for **1**, while the intermolecular interactions, such as those of C–F, C–H, and π–π stacking, were not observed in **5**. In general, effective intermolecular interactions contribute to red-shifted absorption and emission energies, leading to lower band gaps. Therefore, the red-shifted absorption and emission maxima for **2** could be attributed to the increase of π-orbital conjugation between the perfluorocyclopentene and fluorene rings as well as the presence of intermolecular interactions in the solid state. Based on our observations and above elucidations, we believe that the observed red-shifted absorption and emission spectra of compound **1** are likely due to the strong electron-withdrawing effect of the perfluorocyclopentene unit and the more extended conjugation. The PL efficiencies of **1**, **2**, and **4** were noteworthy. It has been well known that DPA (9,10-diphenylanthracene) is regarded as a standard for blue fluorescence with a Φ_{PL} of 0.95.[20] As compared to that of DPA, compounds **1**, **2**, and **4** show high PL quantum efficiency and increase in the order **2**>**1**>**4**>**3**. The extended conjugation and the lack of thermal vibrations caused by strong C–F bonds may be responsible for the enhanced PL efficiencies. To gain a deeper insight into the electronic and luminescent properties, we performed ab initio calculations (level of calculation B3LYP/3-21G*) on **1** and **5** employing the Gaussian 98 package.[21] The geometrical parameters employed in the calculations were taken from their structural data. A contour plot showing the electron density of highest occupied molecular orbitals (HOMO's), second HOMO's, lowest unoccupied molecular orbitals (LUMO's), and second LUMO's for compounds **1** and **5** along with the orbital energy for each levels is depicted in Figure 5. As one may see, the HOMOs and LUMOs of both compounds are similar. The HOMOs of both compounds are dominated by π-orbitals of fluorene but involve some contribution of the π-orbital on the perfluorocyclopentene or benzene moiety. The second HOMO of **1** shows that the π-orbitals of fluorene overlap with the π-orbitals of the ethene unit in the perfluorocyclopentene ring. In contrast, an effective π-orbital overlap between the benzene and fluorene units in the second HOMO level for **5** was not observed. The effective overlap of the HOMO level for **1** certainly should lead to the decrease of the HOMO energy level relative to that of **5**. Although the surfaces of the LUMOs of both compounds are similar (fluorene-based π* orbitals), the π* orbitals contribution of the perfluorocyclopentene ring for **1** is greater than that of the difluorobenzene ring of **5**. It is noteworthy that the perfluorocyclopentene ring greatly influences the LUMO levels, as compared to the benzene moiety. The energy differences between **1** and **5** in the LUMO level is 0.026 Hartree (16.315 kcal/mol), while in the HOMO level

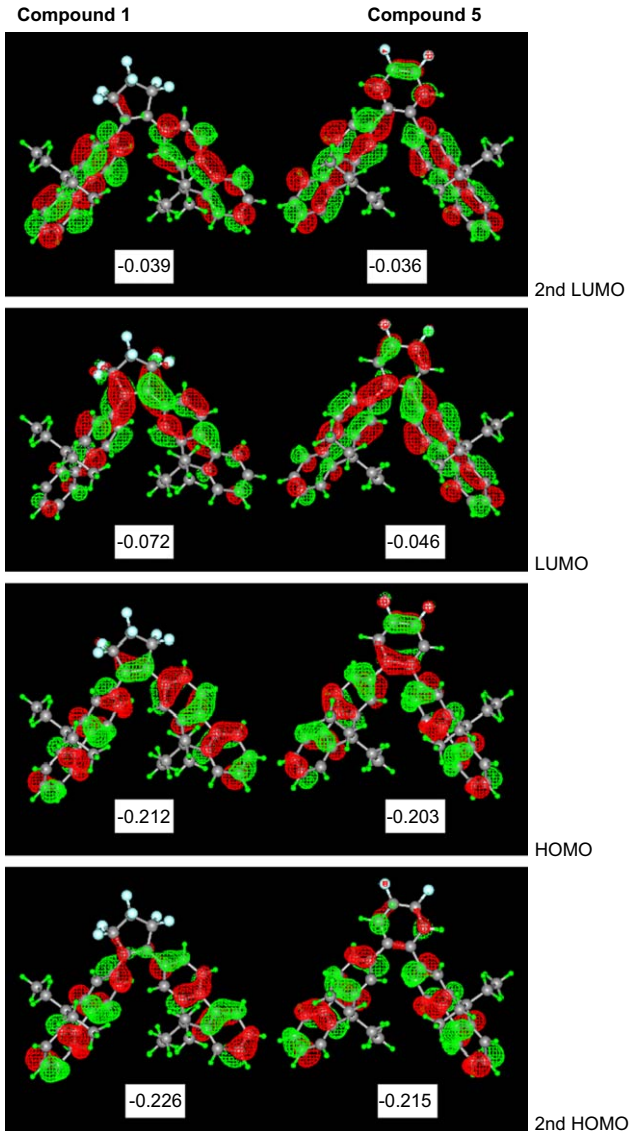

Figure 5. Diagram showing the surfaces and energies of second HOMOs, HOMOs, LUMOs, and second LUMOs for **1** and **5**.

is 0.009 Hartree (5.648 kcal/mol). This result provides support to the evidence that the perfluorocyclopentene unit in **1** plays a key role in the diminution of LUMO energy, bringing about a smaller band gap energy relative to **5**.

The band gaps between the HOMO and LUMO are 3.81 eV (325 nm) for **1** and 4.12 eV (301 nm) for **5**, which are in agreement with their corresponding UV–vis spectra. Judging from these calculations, the luminescence observed in **1**–**4** is indeed believed to originate from fluorene-based π–π* transitions from the perfluorocyclopentene linkage.

2.3. Electroluminescence properties

The electroluminescence (EL) properties of compound **4**, as a representative, were investigated because compound **4** showed high glass-transition temperature. We fabricated a multilayer device with the configuration of ITO/2TNATA (60 nm)/NPB(20 nm)/ADN:2%-compound-**4**(35 nm)/Alq_3 (20 nm)/LiF(2 nm)/Al. The layers of the device consist of

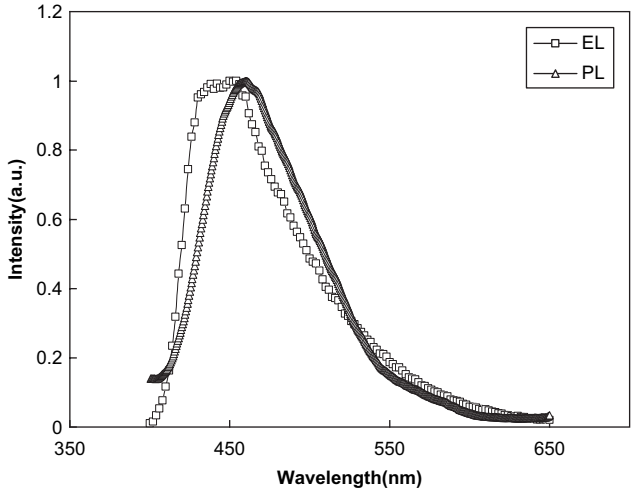

Figure 6. PL (thin film) and EL spectra of **4**. (device structure: ITO/2TNATA(60 nm)/NPB(20 nm)/ADN:2%-compound-**4**(35 nm)/Alq_3(20 nm)/LiF(2 nm)/Al).

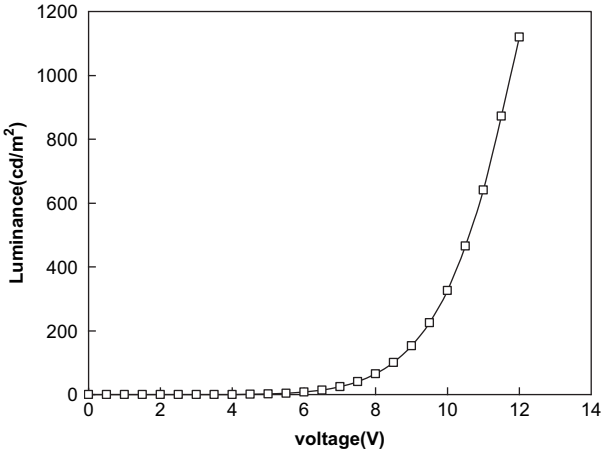

Figure 7. Luminance versus voltage characteristics of **4**-doped devices.

ITO as the anode, 2TNATA as the hole injection layer, NPN as the hole-transporting layer, AND:2%-compound-**4** as the emitter, Alq_3 as the electron transporting layer, LiF as the electron injection layer, and Al as the cathode, respectively. In this study, we chose ADN as the host material, which is a prototypical host with a wide band gap for blue OLEDs. In the EL device, compound **4** displays a blue emission at λ_{max}=458 nm with a shoulder at 438 nm, as shown in Figure 6.

The dominant peak originates from compound **4**, while the shoulder originates from the ADN. The emission observed in the EL device support the suggestion that an incomplete energy transfer from the host to the dopant occurs at the 2 wt %-doped level. The operating voltage (defined as 20 mA/cm^2) of the device is observed at 9 V, which is relatively high. The ability to trap charges in the emissive layer is considered as one of the most important factors in determining the operating voltage.[22] Effective charge trapping by the dopants gives rise to increasing driving voltages in OLEDs. If the dopant material functions as a hole trap, the HOMO level of the dopant could be above that of the host material. In other words, materials having a lower oxidation potential can function as effective hole trapping materials in OLEDs.[27] Therefore, the high operating voltage observed is very likely to stem from the effective hole trapping caused by perfluorocyclopentene unit. The luminescence efficiency of 0.82 cd/A (1120 cd/m^2),with CIE coordinates of x=0.169 and y=0.146, at a current density of 95 mA/cm^2 and a voltage of 12 V was achieved, as shown in Figure 7.

More detailed *I–V–L* characteristics are deposited in electronic supplementary material. The low efficiency in the EL device could be due to the poor of energy transfer between the host and dopant. Although the efficiency is low, we believe that high efficiency should be achieved by changing the concentration of compound **4**. Energy transfers, in general, are quite sensitive upon doping concentration, complete energy transfers tend to emerge at higher doping levels. Further improvement and optimization of EL devices using compound **4** are being investigated in our laboratory.

3. Conclusions

In summary, a series of perfluorocyclopentene-based luminescent compounds have been synthesized and characterized, including their photo- and electroluminescent spectra and electrochemical properties, and the nature of their solid-state structures. The perfluorocyclopentene linkage incorporated with fluorene, anthracene, or spiro-bifluorene moieties can give rise to several distinct characteristics, impacting their solid-state structures, the electrochemical behavior, and photoluminescence. As expected, fluorine atoms on the perfluorocyclopentene ring induce strong intermolecular interaction between two adjacent molecules, leading to high PL efficiency. Moreover, this functional group considerably perturbed the absorption, redox potentials, and photo- and electroluminescent efficiency. In particular, lower HOMO and LUMO energies than those of related compounds were observed, indicating that the perfluorocyclopentene linkage induced a relative ease of hole trapping and the diminution of the band gap. Compound **4**, containing spiro-bifluorene unit, exhibits a bright blue emission in a multilayered EL device.

4. Experimental

4.1. General

All experiments were performed under dry N_2 atmospheres using standard Schlenk techniques. All solvents were freshly distilled over appropriate drying reagents prior to use. The starting materials 2-bromo-9,9′-diethylfluorene, 2-bromo-9,9′-dihexylfluorene, and 2-bromo-9,9′-spirobifluorene were prepared according to the literature procedures.[4] For general experimental details, see the electronic supplementary material.

4.2. Fluorescence quantum yield measurements

The relative quantum yields of PL (Φ_{PL}) for all compounds were determined relative to 9,10-diphenylanthracene (Φ_{PL}=0.95) as the standard in THF or CH_2Cl_2 at 298 K. A range of concentrations of solution of all compounds and standard were measured such that absorbances were less than 0.10 at the excitation wavelength (λ_{ex}=360 nm). The fluorescence

quantum yield was then measured by the previously known process.[14]

4.3. X-ray crystallographic analysis

Suitable crystals of **1** and **5** were obtained from slow vapor diffusion of benzene/hexane (1:1) into solutions of **1** or **5** in CH_2Cl_2. The crystals of **1** and **5** were attached to glass fibers and mounted on a Bruker SMART diffractometer equipped with graphite monochromated Mo Kα (λ= 0.71073 Å) radiation, operating at 50 kV and 30 mA, and a CCD detector; 45 frames of two-dimensional diffraction images were collected and processed to obtain the cell parameters and orientation matrix. All data collections were performed at 173 K. The data collection 2θ ranges for **1** and **5** are 3.32–52.74 and 3.54–56.64, respectively. The first 50 frames were retaken after complete data collection and compared. Both crystals showed no significant decay and no corrections were applied for the decay. The raw data were processed to give structure factors using the SAINT program.[15] Each structure was solved by direction methods and refined by full matrix least squares against F^2 for all data using SHELXTL software (version 5.10).[16] All non-hydrogen atoms in compounds **1** and **5** were anisotropically refined. All hydrogen atoms were placed in idealized positions and refined using a riding model. The crystal system in compound **1** belongs to the monoclinic and $P2_1/c$ space group. One methyl carbon atom of the ethyl groups at the 9-position of the fluorene unit in compound **1** is disordered. The disordered carbon atom was modeled successfully and its contribution to structure factor was included. The crystal system in compound **5** belongs to the triclinic *P*-1 space group. Crystal data for **1** and **5** are summarized in Table 3. The refined atomic coordinates and anisotropic thermal parameters are included electronic supplementary data. Crystallographic data for the structure reported here have been deposited with the Cambridge Crystallographic Data Centre (deposition no. CCDC-609630 for **1**, CCDC-609631 for **5**). The data can be obtained free of charge via http://www.ccdc.cam.ac.uk./perl/catreq/catreq.cgi (or from the CCDC, 12 Union Road, Cambridge CB2 1EZ, UK; fax: +44 1223 336033; e-mail: deposit@ccdc.cam.ac.uk).

Table 3. Crystallographic data for **1** and **5**

	1	**5**
Formula	$C_{39}H_{34}F_6$	$C_{40}H_{36}F_2$
M_W	616.66	554.69
T/K	173(2)	173(2)
Crystal system	Monoclinic	Triclinic
Space group	$P2_1/c$	*P*-1
a/Å	9.5813(4)	8.5214(10)
b/Å	22.8232(10)	11.8260(14)
c/Å	14.6165(6)	15.5735(18)
α/deg		78.631(2)
β/deg	97.4790(10)	83.042(2)
γ/deg		81.673(2)
V/Å^3	3169.1(2)	1515.4(3)
Z	4	2
μ(Mo Kα)/mm^{-1}	0.098	0.077
Crystal size/mm	0.35×0.30×0.30	0.30×0.30×0.20
Reflections collected	18442	9779
Independent reflections	6437	6809
Goodness-of-fit on F^2	1.153	0.992
Final *R*1, *wR*2 [$I>2\sigma(I)$]	0.0770, 0.1638	0.0573, 0.1252
(All data)	0.1007, 0.1752	0.1225, 0.1522

4.4. Fabrication of electroluminescent devices

The glass substrate, pre-coated with indium-tin-oxide (ITO), was cleaned by an ultrasonic bath of acetone, followed by 2-propanol. Surface treatment was carried out by exposing ITO to a UV-ozone plasma. An OLED using AND (9,10-bis(2-naphthyl)anthracene) as host material was fabricated as follows. The hole-injecting layer, a 60 nm thick film of 2TNATA (4,4′,4″-tris[*N*-(2-naphthyl)-*N*-phenylamino)triphenylamine) was deposited on the ITO surface by high vacuum thermal evaporation, and a 20 nm thickness of NPB (*N*,*N*′-di(naphthalen-1-yl)-*N*,*N*′-diphenylbenzidine) as hole-transporting layer was deposited onto the 2TNATA. Compound **4** was 2 wt % doped into a host AND layer by thermal co-evaporation on the NPB layer. A 20 nm thick Alq_3 (tris(8-hydroxyquinolinato)aluminum(III)) layer was then deposited as an electron transporting layer. Finally, LiF (2 nm) and Al (100 nm) were deposited on top of the organic layers by thermal evaporation. The fabricated multilayer organic light-emitting device had the structure of ITO/2TNATA(60 nm)/α-NPB(20 nm)/ADN-compound **4**(35 nm)/Alq_3(20 nm)/LiF(2 nm)/Al(100 nm).

4.5. General syntheses of 1–4

A solution of *n*-BuLi (1.44 mmol, 1.6 M in hexane) was added slowly to the corresponding bromoarenes (1.2 mmol) in THF (25 mL) at −78 °C and stirred for 30 min. To this solution was added octafluorocyclopentene (0.25 mL, 0.6 mmol). Upon addition of octafluorocyclopentene to the lithiated solutions, the color changed rapidly from pale yellow to brown. The reaction mixture was warmed slowly to ambient temperature and stirred overnight. The reaction mixture was poured into water and repeatedly extracted with CH_2Cl_2 (3–50 mL). The combined organic layer was dried over $MgSO_4$, filtered, and concentrated under reduced pressure. The pure corresponding compounds were isolated by chromatographic workup.

4.5.1. 1,2-Bis(9,9′-diethylfluoren-2-yl)-3,3,4,4,5,5-hexafluorocyclopentene (1). Yield: 67% (eluent: hexane, R_f=0.15); mp 113–115 °C MS(EI): *m*/*z*=618 [M]$^+$. ^{1}H NMR ($CDCl_3$, 400 MHz) δ: 7.67–7.65 (2H, m), 7.60 (2H, d, *J*=7.81 Hz), 7.35–7.28 (10H, m), 1.94–1.80 (8H, m), 0.24 (12H, t, *J*=7.34 Hz), ^{13}C NMR ($CDCl_3$, 100 MHz) δ: 150.3, 150.2, 143.5, 140.3, 139.6, 128.4, 128.0, 127.0, 126.5, 123.9, 122.9, 120.1, 119.9, 116.6, 56.2, 32.4, 8.4 (C–F resonances not located). Anal. Calcd for $C_{39}H_{34}F_6$: C, 75.96; H, 5.56. Found: C, 75.81; H, 5.44.

4.5.2. 1,2-Bis(9,9′-dihexylfluoren-2-yl)-3,3,4,4,5,5-hexafluorocyclopentene (2). Yield: 67% (eluent: hexane, R_f=0.35); mp 100–103 °C. MS(EI): *m*/*z*=841 [M]$^+$. ^{1}H NMR ($CDCl_3$, 400 MHz) δ: 7.64–7.62 (2H, m), 7.58 (2H, d, *J*=7.86 Hz), 7.34–7.29 (10H, m), 1.90–1.74 (8H, m), 1.09–1.03 (8H, m), 1.01–0.94 (16H, m), 0.75 (12H, t, *J*=7.07 Hz), 0.52–0.51 (8H, m), ^{13}C NMR ($CDCl_3$, 100 MHz) δ: 151.1, 151.0, 143.1, 139.8, 128.3, 128.0, 126.9, 126.4, 123.8, 122.8, 120.2, 119.9, 55.2, 40.2, 31.5, 29.6, 23.6, 22.5, 13.9 (C–F resonances not located). Anal. Calcd for $C_{55}H_{66}F_6$: C, 78.54; H, 7.91. Found: C, 78.48; H, 7.85.

4.5.3. 1,2-Bis(anthracen-9-yl)-3,3,4,4,5,5-hexafluorocyclopentene (3). The pure compound **3** was obtained by the recrystallization from CH_2Cl_2 and hexane. Yield: 59%; mp 362–364 °C. MS(EI): m/z=528 $[M]^+$. ^1H NMR ($CDCl_3$, 400 MHz) δ: 8.23 (4H, d, J=8.82 Hz), 8.11 (s, 2H), 7.66 (4H, t, J=8.45 Hz), 7.42 (4H, t, J=7.71 Hz), 7.28 (4H, t, J=8.03 Hz), ^{13}C NMR ($CDCl_3$, 100 MHz) δ: 130.7, 130.0, 129.6, 128.9, 128.4, 126.1, 125.2 (C–F resonances not located). Anal. Calcd for $C_{33}H_{18}F_6$: C, 75.00; H, 3.43. Found: C, 74.87; H, 3.39.

4.5.4. 1,2-Bis(9,9′-spirobifluoren-2-yl)-3,3,4,4,5,5-hexafluorocyclopentene (4). Yield: 70% (eluent: ethylacetate/hexane (1/20:v/v), R_f=0.25); mp 275–277 °C. MS(EI): m/z=804 $[M]^+$. ^1H NMR ($CDCl_3$, 400 MHz) δ: 7.82 (2H, d, J=7.66 Hz), 7.73 (4H, d, J=7.63 Hz), 7.60 (2H, d, J=8.02 Hz), 7.40 (2H, t, J=7.49 Hz), 7.25 (6H, t, J=7.11 Hz), 7.15 (2H, t, J=7.51 Hz), 7.08 (4H, t, J=7.50 Hz), 6.66 (2H, d, J=7.59 Hz), 6.55 (4H, d, J=7.53 Hz), 6.50 (2H, s), ^{13}C NMR ($CDCl_3$, 100 MHz) δ: 149.6, 148.8, 147.6, 143.8, 141.5, 140.2, 128.9, 128.7, 127.9, 127.8, 127.7, 126.8, 124.9, 123.9, 123.8, 120.6, 120.2, 119.9, 65.7, 53.4, 31.6, 22.6, 14.1 (C–F resonances not located). Anal. Calcd for $C_{55}H_{30}F_6$: C, 82.08; H, 3.76. Found: C, 82.05; H, 3.59.

4.5.5. Synthesis of 1,2-difluoro-4,5-bis(9,9′-diethylfluoren-2-yl)benzene (5). Aqueous K_2CO_3 (2.0 M, 3.0 mL) and benzyltrimethylammoniumchloride (30.6 mg, 0.165 mmol) were added to a solution of 1,2-dibromo-4,5-difluorobenzene (444.7 mg, 1.648 mmol) and 2-(9,9-diethyl-9H-fluoren-2-yl)-4,4,5,5-tetramethyl-[1,3,2]dioxaborolane (1435 mg, 4.12 mmol) in toluene (17 mL). The mixture was degassed and tetrakis(triphenylphosphine)palladium (76 mg, 4 mol %) was added in one portion under an atmosphere of N_2. The reaction mixture was refluxed for 24 h. After the solution cooled, the solvent was evaporated under vacuum and then extracted with CH_2Cl_2. The solution was washed with brine and H_2O, and then dried over $MgSO_4$. Evaporation of the solvent, followed by column chromatography from hexane, afforded titled product. Yield: 61% (eluent: hexane, R_f=0.15); mp 175–177 °C. MS(EI): m/z=554 $[M]^+$. ^1H NMR ($CDCl_3$, 400 MHz) δ: 7.61–7.59 (2H, m), 7.50 (2H, d, J=8.03 Hz), 7.34 (2H, t, J=9.64 Hz), 7.28–7.26 (6H, m), 1.89–1.75 (8H, m), 0.22 (12H, t, J=7.23 Hz), ^{13}C NMR ($CDCl_3$, 100 MHz) δ: 150.1, 149.8, 141.0, 140.5, 138.5, 137.8, 128.7, 127.1, 126.8, 124.4, 122.8, 119.6, 119.3, 119.3, 119.2, 119.2, 119.1, 56.0, 32.5, 8.5 (C–F resonances not located). Anal. Calcd for $C_{40}H_{30}F_2$: C, 86.61; H, 6.54. Found: C, 86.55; H, 6.59.

Acknowledgements

We thank Dr. Bong Ook, Kim (Gracel Display Inc.) for device fabrication. This research was supported by a grant (F0004021) from Information Display R&D Center, one of the 21st Century Frontier R&D Program funded by the Ministry of Commerce, Industry and Energy of Korean government. This work was partially supported by Korea Research Foundation Grant funded by Korea Government (MOEHRD, Basic Research Promotion Fund) (KRF-2005-015-C00232).

Supplementary data

Supplementary data associated with this article can be found in the online version, at doi:10.1016/j.tet.2006.07.065.

References and notes

1. (a) Paw, W.; Cummings, S. D.; Mansour, M. A.; Connick, W. B.; Geiger, D. K.; Eisenberg, R. *Coord. Chem. Rev.* **1998**, *171*, 125; (b) Cummings, S. D.; Eisenberg, R. *J. Am. Chem. Soc.* **1996**, *118*, 1949; (c) Huertas, S.; Hissler, M.; McGarrah, J. E.; Lachicotte, R. J.; Eisenberg, R. *Inorg. Chem.* **2001**, *40*, 1183; (d) Hissler, M.; Connick, W. B.; Geiger, D. K.; McGarrah, J. E.; Lipa, D.; Lachicotte, R. J.; Eisenberg, R. *Inorg. Chem.* **2000**, *39*, 447.
2. (a) Tang, C. W.; Vanslyke, S. A. *Appl. Phys. Lett.* **1987**, *51*, 913; (b) Baldo, M. A.; O'Brien, D. F.; You, Y.; Shoustikov, A.; Sibley, S.; Thompson, M. E.; Forrest, S. R. *Nature* **1998**, *395*, 151; (c) O'Brien, D. F.; Baldo, M. A.; Thompson, M. E.; Forrest, S. R. *Appl. Phys. Lett.* **1999**, *74*, 442; (d) Kwong, R. C.; Sibley, S.; Dubovoy, T.; Baldo, M. A.; Forrest, S. R.; Thompson, M. E. *Chem. Mater.* **1999**, *11*, 3709; (e) Kwong, R. C.; Laman, S.; Thompson, M. E. *Adv. Mater.* **2000**, *12*, 1134; (f) Chen, C. J.; Shi, J. *Coord. Chem. Rev.* **1998**, *171*, 161; (g) Hu, N. X.; Esteghamatian, M.; Xie, S.; Popovic, Z.; Hor, A. M.; Ong, B.; Wang, S. *Adv. Mater.* **1999**, *11*, 17.
3. (a) Mansour, M. A.; Connick, W. B.; Lachicotte, R. J.; Gysling, H. J.; Eisenberg, R. *J. Am. Chem. Soc.* **1998**, *120*, 1329; (b) Kunugi, Y.; Mann, K. R.; Miller, L. L.; Exstrom, C. L. *J. Am. Chem. Soc.* **1998**, *120*, 589; (c) Fung, E. Y.; Olmstead, M. M.; Vickery, J. C.; Balch, A. L. *Coord. Chem. Rev.* **1998**, *171*, 151; (d) Vickery, J. C.; Olmstead, M. M.; Fung, E. Y.; Balch, A. L. *Angew. Chem., Int. Ed.* **1997**, *36*, 1179; (e) De Santis, G.; Fabbrizzi, L.; Licchelli, M.; Poggi, A.; Taglietti, A. *Angew. Chem., Int. Ed.* **1996**, *35*, 202; (f) de Silva, A. P.; Gunaratne, H. Q. N.; Rice, T. E. *Angew. Chem., Int. Ed.* **1996**, *35*, 2116; (g) Houlne, M. P.; Agent, T. S.; Kiefer, G. F.; McMillan, K.; Bornhop, D. J. *Appl. Spectrosc.* **1996**, *10*, 225; (h) Wong, K. H.; Chan, M. C. W.; Che, C. M. *Chem.—Eur. J.* **1999**, *5*, 2845; (i) Wong, W. Y.; Choi, K. H.; Cheah, K. W. *J. Chem. Soc., Dalton Trans.* **2000**, 113; (j) Liu, H. Q.; Cheung, T. C.; Che, C. M. *Chem. Commun.* **1996**, 1039; (k) Pang, J.; Marcotte, E. J.-P.; Seward, C.; Brown, R. S.; Wang, S. *Angew. Chem., Int. Ed.* **2001**, *40*, 4042.
4. Liu, X.-M.; He, C.; Huang, J.; Xu, J. *Chem. Mater.* **2005**, *17*, 434 and references cited therein.
5. (a) Saitoh, A.; Yamada, N.; Yashima, M.; Okinaka, K.; Senoo, A.; Ueno, K.; Tanaka, D.; Yashiro, R. *SID 04 Digest* **2004**, *35*, 150; (b) Shen, W.-J.; Dodda, R.; Wu, C.-C.; Wu, F.-I.; Liu, T.-H.; Chen, C. H.; Shu, C.-F. *Chem. Mater.* **2004**, *16*, 930; (c) Kim, Y.-H.; Shin, D.-C.; Kwon, S.-K. *Adv. Mater.* **2001**, *13*, 1690; (d) Li, Y.; Fung, M. K.; Xie, Z.; Lee, S.-T.; Hung, L.-S.; Shi, J. *Adv. Mater.* **2002**, *14*, 1317; (e) Shih, H.-T.; Lin, C.-H.; Shih, H.-H.; Cheng, C.-H. *Adv. Mater.* **2002**, *14*, 1409; (f) Danel, K.; Huang, T.-H.; Lin, J. T.; Tao, Y.-T.; Chuen, C.-H. *Chem. Mater.* **2002**, *14*, 3860; (g) Tao, S. L.; Hong, Z. R.; Peng, Z. K.; Ju, W. G.; Zhang, X. H.; Wang, P. F.; Wu, S. K.; Lee, S. T. *Chem. Phys. Lett.* **2004**, *397*, 1; (h) Benmansour, H.; Shioya, T.; Sato, Y.; Bazan, G. C. *Adv. Funct. Mater.* **2003**, *13*, 883; (i) Shi, J.; Tang, C. W. *Appl. Phys. Lett.* **2002**, *80*, 3201; (j) Tao, S.; Peng, Z.; Zhang, X.; Wang, P.; Lee, C.-S.; Lee, S.-T. *Adv. Funct. Mater.* **2005**, *15*, 1716.

6. (a) Hung, L. S.; Chen, C. H. *Mater. Sci. Eng. R.* **2002**, *39*, 143 and references cited therein; (b) *Organic Electroluminescent Materials and Derivatives*; Miyata, S., Nalwa, H. S., Eds.; Gordan and Breach: New York, NY, 1997; (c) Hide, F.; Diaz-Garcia, M. A.; Schartz, B. J.; Heeger, A. J. *Acc. Chem. Res.* **1997**, *30*, 430.
7. Vamvounis, G.; Schulz, G. L.; Holdcroft, S. *Macromolecules* **2004**, *37*, 8897.
8. Lee, J. H.; Hwang, D. H. *Chem. Commun.* **2003**, 2836.
9. Shi, J.; Tang, C. W. *Appl. Phys. Lett.* **1997**, *70*, 1665.
10. An, B.-K.; Lee, D.-S.; Lee, J.-S.; Park, Y.-S.; Song, H.-S.; Park, S. Y. *J. Am. Chem. Soc.* **2004**, *126*, 10232.
11. (a) Heidenhain, S. B.; Sakamoto, Y.; Suzuki, T.; Miura, A.; Fujikawa, H.; Mori, T.; Tokito, S.; Taga, Y. *J. Am. Chem. Soc.* **2000**, *122*, 10240; (b) Sakamoto, Y.; Suzuki, T.; Miura, A.; Fujikawa, H.; Mori, T.; Tokito, S.; Taga, Y. *J. Am. Chem. Soc.* **2000**, *122*, 1832.
12. Kang, Y.; Park, K.-M.; Kwon, S.-K.; Ko, J. *Mol. Cryst. Liq. Cryst.* **2006**, *444*, 157.
13. (a) Irie, M. *Chem. Rev.* **2000**, *100*, 1685 and references cited therein; (b) Tsujioka, T.; Masuda, K. *Appl. Phys. Lett.* **2003**, *83*, 4978; (c) Tsujioka, T.; Kondo, H. *Appl. Phys. Lett.* **2003**, *83*, 937.
14. Demas, J. N.; Crosby, G. A. *J. Phys. Chem.* **1971**, *75*, 991.
15. *Bruker, SMART and SAINT: Area Detector Control and Integration Software Ver. 5.0*; Bruker Analytical X-ray Instruments: Madison, WI, 1998.
16. *Bruker, SHEXTL: Structure Determination Programs Ver. 5.16*; Bruker Analytical X-ray Instruments: Madison, WI, 1998.
17. Lee, S. H.; Jang, B.-B.; Kafafi, Z. H. *J. Am. Chem. Soc.* **2005**, *127*, 9071.
18. Choi, H.; Lee, H.; Kang, Y.; Kim, E.; Kang, S. O.; Ko, J. *J. Org. Chem.* **2005**, *70*, 8291.
19. Salbeck, J.; Yu, N.; Bauer, J.; Weissortel, F.; Estgen, H. *Synth. Met.* **1997**, *91*, 209.
20. Lakowicz, J. R. *Principles of Fluorescence Spectroscopy*; Kluwer Academic: New York, NY, 1996.
21. Frisch, M. J., et al. *Gaussian 98, revision A6*; Gaussian: Pittsburgh, PA, 1999.
22. (a) Lane, P. A.; Palilis, L. C.; O'Brien, D. F.; Giebeler, C.; Cadby, A. J.; Lidzey, D. G.; Campbell, A. J.; Blau, W.; Bradley, D. D. C. *Phys. Rev. B* **2001**, *63*, 235206; (b) O'Brien, D. F.; Giebeler, C.; Fletcher, R. B.; Cadby, A. J.; Palilis, L. C.; Lidzey, D. G.; Lane, P. A.; Bradley, D. D. C.; Blau, W. *Synth. Met.* **2001**, *116*, 379; (c) Gong, X.; Ostrowski, J. C.; Moses, D.; Bazan, G. C.; Heeger, A. J. *Adv. Funct. Mater.* **2003**, *13*, 439; (d) Nuesch, F.; Berner, D.; Tutis, E.; Schaer, M.; Ma, C.; Wang, X.; Zhang, B.; Zuppiroli, L. *Adv. Funct. Mater.* **2005**, *15*, 323.